Empirical Estimation of Attenuation from Differential Propagation Phase Measurements at C Band

JONATHAN J. GOURLEY,* PIERRE TABARY, AND JACQUES PARENT DU CHATELET

Direction des Systèmes d'Observation, Météo-France, Trappes, France

(Manuscript received 24 November 2005, in final form 11 July 2006)

ABSTRACT

A polarimetric method is devised to correct for attenuation effects at C band on reflectivity Z_H and differential reflectivity Z_{DR} measurements. An operational cross-correlation analysis is used to derive advection vectors and to displace echoes over a 5-min time step. These advected echoes are then compared with observations valid at the same time. The method assumes that the mean change in the intrinsic Z_H and Z_{DR} over a 5-min period when considering 1–2 h of observations over the entire radar umbrella is approximately zero. Correction coefficients are retrieved through the minimization of a cost function that links observed decreases in Z_H and Z_{DR} due to attenuation effects with increases in differential phase shift (Φ_{DP}). The retrieved coefficients are consistent with published values for the typical ranges of temperatures and drop sizes encountered at midlatitudes, even when Mie scattering effects are present. Measurements of Z_H and Z_{DR} corrected using retrieved coefficients are compared with raw measurements and to measurements adjusted by mean coefficients found in the literature. The empirical retrieval method shows improvement over using mean correction coefficients based on comparisons of Z_H from neighboring, unattenuated radars, disdrometer measurements, and analysis of Z_H and Z_{DR} as a function of Φ_{DP}.

1. Introduction

Improved sensitivity and relatively lower costs of radars operating at C-band frequencies may be partially offset by their susceptibility to attenuation that can significantly reduce values of reflectivity at horizontal polarization Z_H and differential reflectivity Z_{DR}, thus affecting the quality of rainfall measurements. Attenuation correction methods that rely on Z_H measurements alone have proven to be unreliable. Hitschfeld and Bordan (1954) proposed a scheme based on an empirical relationship between the specific horizontal attenuation A_H and Z_H. Although Aydin et al. (1989) and Gorgucci et al. (1995, 1998) suggested accuracies of gate-to-gate corrections up to 10%, these profiling schemes are notoriously unstable because any initial error in Z_H due to a slight miscalibration grows very rapidly.

Bringi and Chandrasekar (2001) provide an excellent summary of methods to correct for attenuation of Z_H and Z_{DR} at attenuating frequencies using the phase difference Φ_{DP} between horizontally (H) and vertically (V) polarized returns. These measurements have the advantage of being immune to radar miscalibration (Zrnić and Ryzhkov 1996). As raindrops grow they become more oblate, leading to positive values of Z_{DR}, and the slower velocity of the H wave relative to V leads to a value of Φ_{DP} that increases with range in a rainfall medium. Scattering simulations assuming gamma functions for raindrop size distributions suggested that the attenuation A_h and differential attenuation A_{HV} are nearly linearly related to the gradient of Φ_{DP} with range in degrees per kilometer or specific differential phase K_{DP} at X, C, and S bands by coefficients a and b, respectively (Bringi et al. 1990). These coefficients can vary because of changes in drop tem-

* Current affiliation: NOAA National Severe Storms Laboratory/National Weather Center, Norman, Oklahoma.

Corresponding author address: Dr. Jonathan J. Gourley, Research Hydrometeorologist, National Severe Storms Laboratory/National Weather Center, 120 David L. Boren Blvd., Rm. 4745, Norman, OK 73072-7303.
E-mail: jj.gourley@noaa.gov

DOI: 10.1175/JAM2464.1

perature, nonuniqueness of drop aspect ratio–drop size relation, variability in drop size distribution details, and Mie scattering effects (Jameson 1992; Carey et al. 2000; Matrosov et al. 2002, 2005).

Ryzhkov and Zrnić (1995) produced scatterplots of Φ_{DP} versus Z_H and Φ_{DP} versus Z_{DR} using a large dataset collected at S band. The slope of the fitted lines yielded values of a and b that were larger than those of Bringi et al. (1990), which they attributed to additional attenuation due to Mie scattering. Carey et al. (2000) adapted the technique of Ryzhkov and Zrnić (1995) for C-band radar by identifying rays with Mie scattering effects (equivolumetric median diameter drops > 2.5 mm or Z_{DR} > 2.5–3 dB at C band) where larger coefficients (2 times as large for a and 4 times as large for b!) were applied to these rays if they had large backscatter differential phase δ, dips in the copolar cross-correlation coefficient at zero time lag [$\rho_{HV}(0)$], and high values of K_{DP}. Ranges of K_{DP} are also used to limit the data sample so that the intrinsic scatter in Z_{DR} and Z_H at a given value of Φ_{DP} is minimized.

Smyth and Illingworth (1998) proposed a method at C band based on constraining values of Z_{DR} behind intense convective cells where the intrinsic Z_{DR} was believed to be 0 dB, representing spherical droplets. Observations of negative Z_{DR} were used to correct for horizontal and differential attenuation effects; the total differential attenuation was then redistributed to gates along the radial with $K_{DP} > 1°$ km^{-1}, yielding an estimate of A_{HV}. A linear relationship was then assumed between A_{HV} and A_h based on scattering simulations, thus providing for a correction to values of Z_H and Z_{DR}. This method offers the advantage of being applied on a ray-by-ray basis. However, the constraint of an intrinsic Z_{DR} of 0 dB in drizzle regions, for which the method is based, is difficult to identify automatically using other polarimetric parameters. In addition, the approach is susceptible to nonuniform beam-filling effects on Z_{DR} measurements near the edges of convection.

The "ZPHI" algorithm (Testud et al. 2000) is similar in design to the original technique of Hitschfeld and Bordan (1954), with the additional constraint of estimating the reference attenuation at C band. The Φ_{DP} constraint leads to numerical stability, which was the main failing with the original technique. The ZPHI algorithm may yield inaccurate results because of deviations from the assumed raindrop size–shape model and in situations where the observed Φ_{DP} is small relative to system noise levels. Also, Z_H values become biased along with the estimated A_H if measurements from hail or mixed-phase hydrometeors are included in the calculations. This method has been modified by adding a combined Φ_{DP}–Z_{DR} constraint as described in Bringi and Chandrasekar (2001, their section 7.4) and has been adapted for use at X band (Iwanami et al. 2003; Anagnostou et al. 2004; Park et al. 2005a).

A new approach is proposed herein that seeks a solution to the coefficients a and b linking attenuation of Z_H and Z_{DR} to observations of Φ_{DP}. The technique is empirical and is based on the assumption that the mean, intrinsic difference between cross-correlated Z_H (Z_{DR}) data over a 5-min period is approximately zero when a sufficiently large number of observations are considered. Reductions in Z_H (Z_{DR}) are shown to be linearly related to increases in Φ_{DP}, which are used to solve for the a and b coefficients. Coefficients are retrieved for seven cases of intense convection occurring near Météo-France's C-band polarimetric radar. Evaluations are made possible by comparing raw measurements with measurements adjusted using mean coefficients found in the literature, and to corrected Z_H and Z_{DR} values using empirically retrieved coefficients.

The conceptual basis and mathematical background of the technique are described in section 2. Section 3 presents results of the retrieved curves. The variability of these curves from case to case is also examined in this section. Section 4 evaluates the accuracy of the method by examining the behavior of Z_H and Z_{DR} as a function of Φ_{DP} with uncorrected data, data corrected using mean coefficients, and data corrected using retrieved coefficients. The methods are also objectively evaluated using comparisons with unattenuated data from neighboring radars and disdrometer measurements. A summary of results and conclusions are presented in section 5. The final section also discusses operational aspects of the algorithm, including its limitations and potential improvements.

2. Description of method to retrieve attenuation and differential attenuation coefficients to correct radar signals at C band

a. *Conceptual overview*

The retrieval technique was envisioned based on observations of Z_{DR}, and to a lesser extent Z_H, as intense convective cells moved near the Trappes, France, radar. Strong rain cells at close range were noted to have the effect of producing wedge-shaped artifacts of anomalously low Z_{DR} values at ranges beyond the initial, attenuating cell. These wedges would often propagate in the azimuthal direction with respect to the radar, creating the appearance of a moving searchlight. Images of Z_H also revealed these artifacts, yet they were harder to

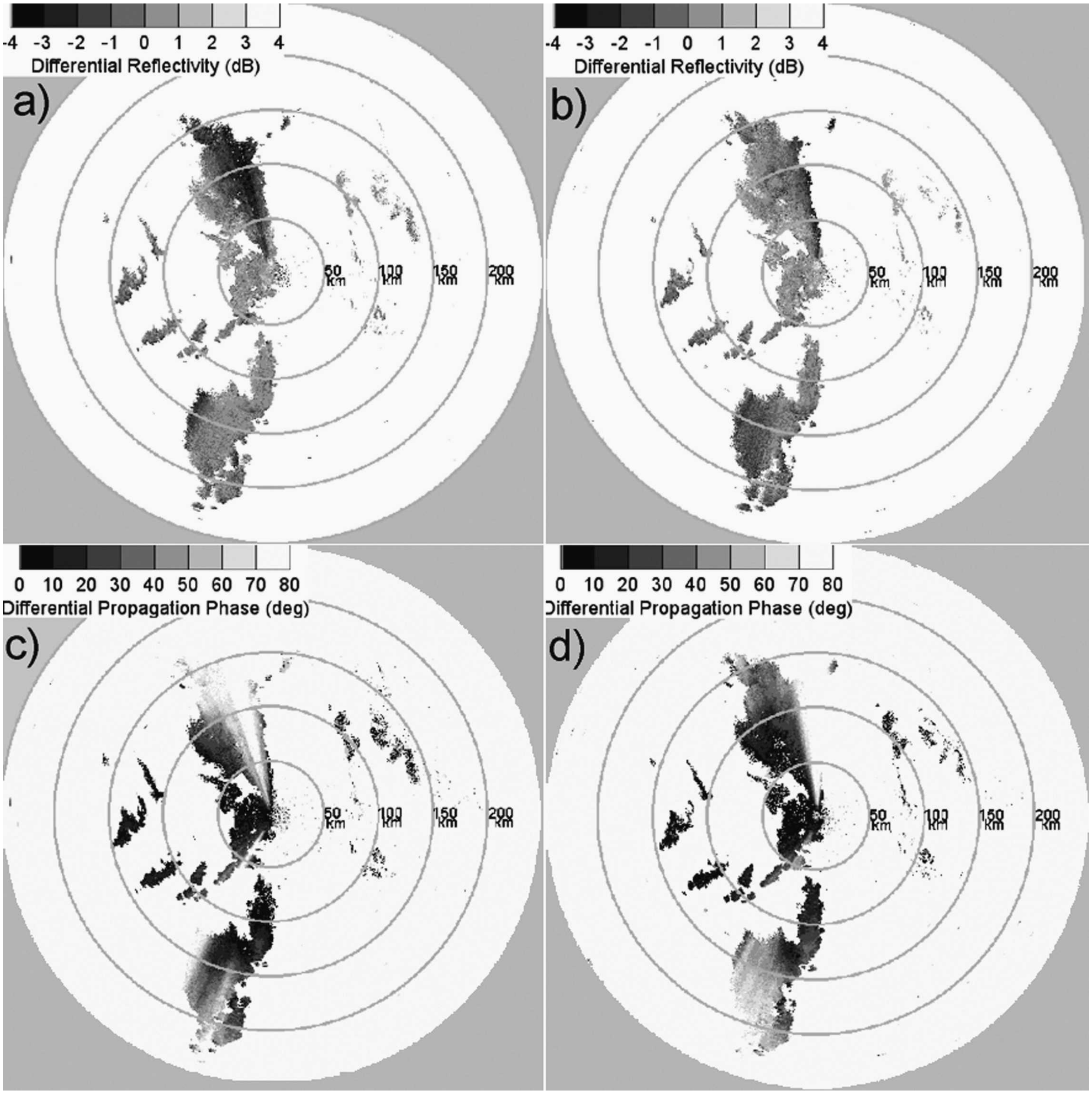

FIG. 1. An example at 1700 UTC 24 Mar 2005 showing (a) Z_{DR} values from a previous scan that have been advected over a 5-min time step so that they can be compared with (b) observed values of Z_{DR}. The mean changes in Z_{DR} are coupled to changes in Φ_{DP} between (c) advected and (d) observed data to solve for the b coefficient.

discern 1) because of the higher variability of Z_H in attenuated regions as compared with Z_{DR} and 2) because attenuation reduces Z_{DR} values more substantially per unit Z_{DR} as compared with Z_H. Because these artifacts were moving quickly from scan to scan, it occurred that it would be possible to advect Z_H (Z_{DR}) data from a previous scan so that the data were matched in space in time. Mean differences are assumed to be due to attenuation and are thus linked to differences in Φ_{DP} measurements between advected and observed images.

Figure 1 illustrates the empirical retrieval concept developed herein using two scans of Z_{DR} and Φ_{DP} at an elevation angle of 1.5°, where the data from the first scan have been advected using an operational cross-correlation analysis so they match the data in the second scan. A wedge of negative Z_{DR} values is evident northwest of the radar (Fig. 1a) that was the result of an intense convective cell very near the radar. After 5 min the cell moved north of the radar so that the wedge of attenuated Z_{DR} data moved clockwise with respect to the radar, resembling a moving searchlight (Fig. 1b). Figure 1c shows that this wedge of attenuated Z_{DR} was coincident with large values of Φ_{DP}. Large Φ_{DP} values also rotated in a searchlight pattern to the north of the radar (Fig. 1d). If we assume for simplicity that the Z_{DR} data to the northwest of the radar were from spherically shaped drops that changed from being attenuated (−5 dB) to unattenuated (0 dB), then these increases can be linked to reductions in Φ_{DP} from 100° to 0°, for example. In this case, we can say that a gain of 5 dB in Z_{DR} was caused by a loss of 100° in Φ_{DP}, so that the *b* coefficient is 0.02. However, such a direct solution at a particular grid point is subject to errors caused by intrinsic, microphysical changes within a 5-min period.

Thousands of comparisons are available using each Z_H, Z_{DR} pair from a series of radar scans. A data pair refers to the advected and observed values of Z_H and Z_{DR} at a given grid point. Mean differences in the *intrinsic* Z_{DR} and Z_H between the advected and observed images are assumed to be zero when considering thousands of data pairs under the radar umbrella over a 1–2-h duration. Changes in a 5-min period do occur at a given pixel because of precipitation growth, decay, or microphysical processes. However, the net change over the entire spatial/temporal domain is assumed to be zero. In other words, it is equally probable that a given precipitation feature will change intrinsically because of growth or decay, and the net change when considering thousands of pairs is thus zero.

Raw measurements of Z_H, Z_{DR}, copolar cross-correlation coefficient at zero time lag $\rho_{HV}(0)$, and Φ_{DP} from the Trappes radar are subject to errors resulting from miscalibration, near-radome interference effects, and noise. For details regarding an examination of each of these effects, proposed correction techniques, and a summary of the data quality of the Trappes polarimetric radar, see Gourley et al. (2006). In summary, structures in the near field of the antenna were found to affect Z_{DR} measurements by as much as 0.4 dB. An empirical mask was developed and subsequently applied to all Z_{DR} data used in this study. Biases in Z_{DR} and $\rho_{HV}(0)$ measurements that occur at signal-to-noise values of less than 10 dB have been mitigated. Measurements of Z_{DR} have been calibrated using observations at vertical incidence where the intrinsic Z_{DR} is known to be 0 dB. The behavior of initial differential phase measurements with the Trappes radar has been examined, and it was found that raw measurements are aliased, vary with azimuth, and have a mean offset of 6°. An empirical equation was developed to correct Φ_{DP} measurements for the initial system offset and has subsequently been applied to all Φ_{DP} measurements used in this study.

Thresholds are applied to the data pairs so that errors from brightband contamination, ground clutter, hail contamination, and noisy Φ_{DP} measurements in light rain are mitigated. Values of $\rho_{HV}(0)$ were observed to decrease below 0.97 within the melting layer. Thus, data pairs are discarded from the retrieval method if they have values of $\rho_{HV}(0)$ less than 0.97. This threshold also eliminates many Z_H and Z_{DR} measurements affected by ground clutter. Data must be collected within 5–150 km from radar to reduce ground clutter and brightband contamination further. Measurements in hail are avoided by thresholding maximum Z_H values at 40 dB*Z*. Noisy Φ_{DP} measurements are first mitigated by smoothing Φ_{DP} profiles along a 25-gate window corresponding to 6 km. Second, the difference in Φ_{DP} between advected and observed data pairs must be more than 10° so that the comparisons are made well above the measurement noise level of 1.8° found with the Trappes radar (Gourley et al. 2006).

The developed method is dependent on motion vectors derived from a cross-correlation analysis that is used to displace Z_H, Z_{DR}, and Φ_{DP} data forward in time by 5 min. The cross-correlation technique is very similar to the Tracking Radar (or Reflectivity) Echoes by Correlation (TREC) developed by Rinehart (1979) and later modified by Tuttle and Foote (1990). An array of reflectivity data within a 60 × 60 km^2 area is correlated with a second array of reflectivity data separated by 5 min. The displacement between the initial array location and that of the array having the largest correlation coefficient determines the motion vector. These derived motion vectors are then used to advect the echoes forward in time by 5 min. Errors in the motion vectors will cause the data initially separated by 5 min to be mismatched. In this case, differences in Z_H (Z_{DR}) for a given difference in Φ_{DP} will not be due to attenuation but rather to displacement. The effect on the retrieved coefficients depends on the structure of the precipitation relative to the biases in the motion vectors, but in general the retrieved coefficients are expected to be normally distributed around a mean value of zero.

It should be noted that the retrieval technique does not require that one of the measurements remain completely free from attenuation effects. It is the mean *difference* in Z_H (Z_{DR}) between measurements that have been advected over a 5-min period and observed data that is of interest to the algorithm. A relationship is assumed between domainwide Z_H (Z_{DR}) differences per unit change in Φ_{DP}, thus providing for the computation of the *a* (*b*) coefficient.

b. Mathematical background

The goal of this analysis is to derive empirically the coefficients a and b that link the observed Φ_{DP} to the attenuation of Z_H and Z_{DR}. For simplicity, the development presented here is for Z_H and is completely analogous to the treatment of Z_{DR}. It is first assumed that the measured reflectivity Z_H is related to the intrinsic reflectivity as follows:

$$Z_H = Z_H^{\text{int}} - a\Phi_{DP}, \tag{1}$$

where a is the coefficient for horizontal attenuation [dB $(°)^{-1}$]. Because (1) relies on an absolute measure of Φ_{DP}, measurements have been dealiased and corrected for the initial system offset as discussed in section 2a.

Next, we assume the relationship in (1) holds for measured reflectivity that has simply been advected in space over a 5-min time step, so that

$$\hat{Z}_H = \hat{Z}_H^{\text{int}} - a\Phi_{DP}, \tag{2}$$

where the hat symbol refers to values that were *advected* using cross-correlation analysis. With this, we can combine (1) and (2) as follows:

$$Z_H - \hat{Z}_H = -a(\Phi_{DP} - \Phi_{DP}). \tag{3}$$

From (3), it is theoretically possible to estimate a at a single grid point. However, this estimate is likely to be associated with a large degree of error resulting from intrinsic microphysical changes that occur over 5 min. A better estimate is accomplished when the entire number of measurements n subject to the thresholds discussed in section 2a is considered. Thus, (3) is rewritten in matrix form:

$$Z_H(i) - \hat{Z}_H(i) = (-1, 0, 0, 0, 0, 0, 0, 0, 0, 1, \ldots) \cdot \left.\begin{pmatrix} -A(0) \\ -A(1) \\ \ldots \\ -A(360) \end{pmatrix}\right|_{i=1}^{n}, \tag{4}$$

where, in the example shown in (4), Φ_{DP} values occupy the 1st and 10th position element, meaning the observed and advected Φ_{DP} values were 0° and 10°, respectively. The 360 elements correspond to all possible Φ_{DP} values ranging from 0° to 360°. This enables the total attenuation A to be computed as a function of Φ_{DP}. This calculation is repeated over all n measurements corresponding to all ranges and azimuths for a 1–2-h duration. Equation (4) is more easily represented in the following matrix system:

$$\mathbf{Z} - \hat{\mathbf{Z}} = \overline{\mathsf{PHI}} \cdot (-\mathbf{A}), \tag{5}$$

where observed and advected reflectivity vectors $\mathbf{Z}$ contain n elements, $\overline{\mathsf{PHI}}$ is an $n \times 360$ matrix, and $\mathbf{A}$ is a 360-element vector corresponding to the coefficients. Because the system is overdetermined ($n \gg 360$), the following cost function $\mathbf{J}$ is introduced:

$$\mathbf{J} = [\mathbf{Z} - \hat{\mathbf{Z}} - \overline{\mathsf{PHI}} \cdot (-\mathbf{A})]^{\mathrm{T}} \cdot [\mathbf{Z} - \hat{\mathbf{Z}} - \overline{\mathsf{PHI}} \cdot (-\mathbf{A})] + \boldsymbol{\lambda}^{\mathrm{T}}[\mathbf{U}^{\mathrm{T}} \cdot (-\mathbf{A})] \cdot [\mathbf{U}^{\mathrm{T}} \cdot (-\mathbf{A})], \tag{6}$$

where the superscript T refers to the transpose of the matrix. To make the retrieval well posed, a term involving $\mathbf{U}$ is added to the cost function imposing the first element of $\mathbf{A}$ to be 0 (i.e., there is no attenuation if Φ_{DP} is equal to zero). The vector $\mathbf{U}$ is composed of 360 elements, where the first is equal to 1 and the remaining ones are set to 0. The weight of this constraint is controlled by setting a very large value for $\boldsymbol{\lambda}$. The cost function $\boldsymbol{J}$ is minimized with respect to $\boldsymbol{A}$ in a least squares sense as follows:

$$\mathbf{A} = -[(\overline{\mathsf{PHI}}^{\mathrm{T}} \cdot \overline{\mathsf{PHI}} - \lambda\mathbf{U}^{\mathrm{T}} \cdot \mathbf{U})^{-1} \cdot \overline{\mathsf{PHI}}^{\mathrm{T}} \cdot (\mathbf{Z} - \hat{\mathbf{Z}})]. \tag{7}$$

This method provides for the retrieval of the total attenuation (total differential attenuation) in decibels at all 360 values of Φ_{DP}. If linearity is assumed, then slopes of lines fit to the retrieved path-integrated attenuation (differential attenuation) as a function of Φ_{DP} correspond to the coefficients a (b) used to correct observations of Z_H (Z_{DR}). The following section examines this linearity assumption and the variability of retrieved coefficients with Φ_{DP}.

3. Results from attenuation and differential attenuation retrievals

a. Case studies

The technique of retrieving coefficients for attenuation using advected fields of Z_H and Z_{DR} is tested here for seven cases of intense convection. As seen in Table 1, a very large sample size is produced using as few as 12 scans (one hour's worth) at an elevation angle of 1.5°. Figures 2a,b show the path-integrated attenuation and differential attenuation plotted as a function of

TABLE 1. Summary of event dates and times, sample sizes, and retrieved attenuation correction coefficients [dB $(°)^{-1}$] a ($=A_H/K_{DP}$) and b ($=A_{HV}/K_{DP}$) at C band.

Date	Event start–end times (UTC)	Sample size	a	b
24 Mar 2005	1600–1800	6.95×10^5	0.0805	0.0304
03 Jun 2005	1400–1600	7.97×10^4	0.1111	0.0311
23 Jun 2005	1500–1700	1.62×10^6	0.1044	0.0496
26 Jun 2005	1000–1100	1.01×10^6	0.0817	0.0268
28 Jun 2005	2000–2100	1.04×10^6	0.0719	0.0294
30 Jun 2005	1500–1700	1.61×10^6	0.0737	0.0336
04 Jul 2005	0400–0500	1.76×10^6	0.0300	0.0166

Φ_{DP}. Linear least squares regression is then used to fit a line to each curve and obtain the slope; these slopes are the retrieved coefficients and are summarized in Table 1. The thick gray lines in Figs. 2a,b correspond to the expected minimum and maximum correction coefficients at C band as reported in Carey et al. (2000). The minimum values come from scattering simulations, and the maxima are the empirical coefficients found by Carey et al. (2000) that account for increasing slopes resulting from the presence of large-diameter drops in convective cores.

The curves that were retrieved for attenuation of Z_H (Fig. 2a) nearly fall within the expected bounds. The 4 July 2005 case suggests there is the least amount of attenuation, and the 3 and 23 June 2005 cases indicate the most (refer to Table 1). The variability of these curves from case to case is examined in the next section. All curves describing the path-integrated differential attenuation (Fig. 2b) fall within expected bounds. These curves are better approximated as being linear and are smoother than those shown in Fig. 2a. The following section examines whether the different a and b coefficients that were retrieved are related to the presence of large drops or different temperatures in the attenuating cells.

b. Variability of retrieved correction coefficients

Attenuation effects on Z_H and Z_{DR} enhance as equivolume median diameters D_o enter the Mie scattering regime at approximately 2.5 mm at C band (Carey et al. 2000). Simulations have also shown that the temperature of the raindrops, DSD variability, and raindrop-axis-ratio relation affect the relationship between attenuation and Φ_{DP} (Jameson 1992; Matrosov et al. 2002, 2005). The Carey et al. method improves over the original technique of Ryzhkov and Zrnić (1995) by accounting for the variability of a and b due to large drops resulting in Mie scattering. Although

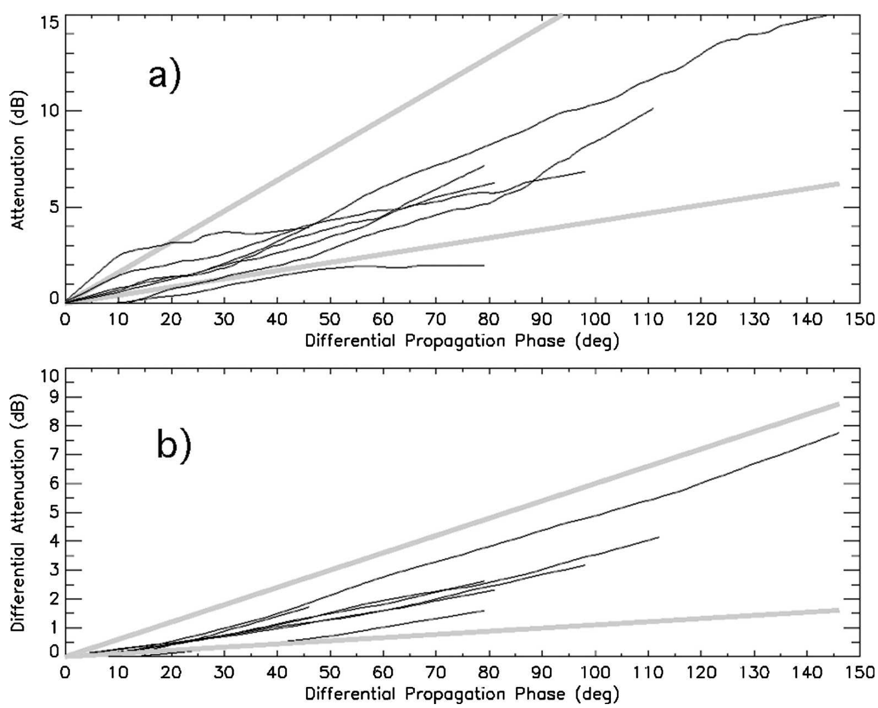

FIG. 2. Retrieved curves (in black) of Φ_{DP} vs (a) path-integrated attenuation and (b) path-integrated differential attenuation for seven cases of intense convection listed in Table 1. The slopes of the gray lines correspond to the minimum and maximum correction coefficients published in simulation-based and empirical studies.

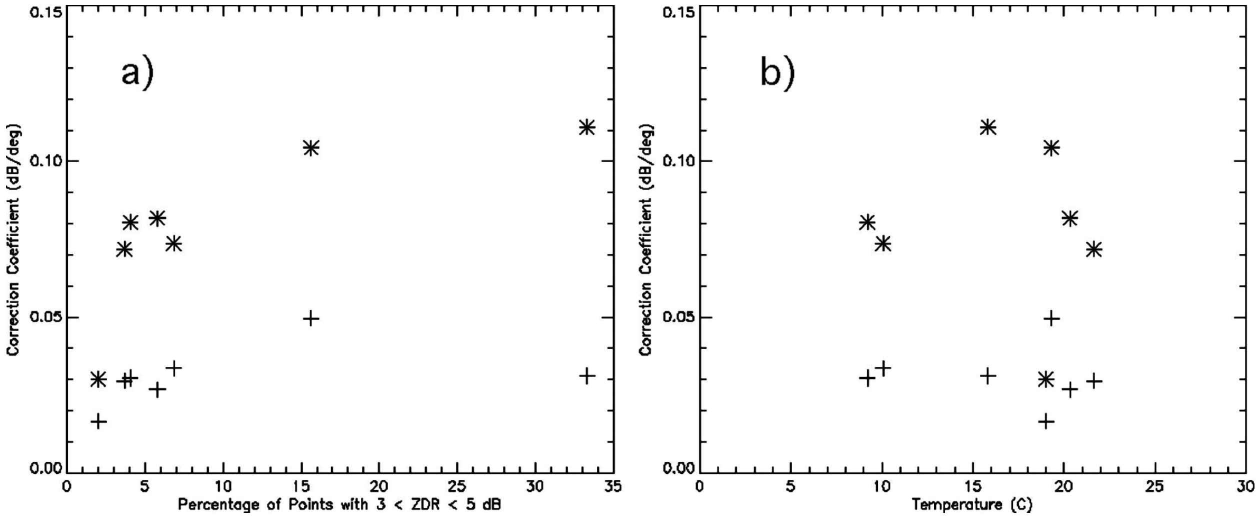

FIG. 3. Sensitivity of correction coefficients [dB $(°)^{-1}$] a ($=A_H/K_{DP}$; asterisks) and b ($=A_{HV}/K_{DP}$; plus signs) to (a) percentage of cells with $3 < Z_{DR} < 5$ dB and to (b) temperature. Cells must have $\Phi_{DP} < 10°$, $\rho_{HV}(0) > 0.90$, and $Z_H > 40$ dBZ.

simulations indicate that a and b are sensitive to the assumed drop shape model, Matrosov et al. (2005) note that the slope of the drop-axis-ratio relation is fairly constant except for drops with diameters larger than 7 mm. The retrieval method developed herein is empirical; therefore, separating these effects is not unambiguous.

The Z_{DR} polarimetric variable responds well to hydrometeor shapes, sizes, and habits, and therefore it can be used to detect the presence of large drops ($3 < Z_{DR} < 5$ dB at C band) provided that the Z_{DR} data are not attenuated. To avoid attenuated Z_{DR} values, a threshold of $\Phi_{DP} < 10°$ is implemented so that the analysis is effectively restricted to portions of cells that are either close to the radar or have very little precipitation between them and the radar. The percent of unattenuated data having Z_{DR} values within the Mie scattering regime is reported. The temperatures of these cells are also determined by utilizing radiosonde observations launched at the Trappes radar site.

Figure 3a shows the retrieved a and b coefficients plotted against the percent of unattenuated cells containing big drops for all cases listed in Table 1. Although the data sample is small, both coefficients exhibit a nonlinear dependence on the presence of big drops within these cells. Increases in a and b are most significant up to percentages of 10% and level off thereafter. The drop size dependence of relationships between attenuation and Φ_{DP} cannot be neglected. The processes resulting in high sensitivity of a and b to drop sizes are either Mie scattering effects or changes in the drop-axis-ratio relation. Regardless of the mechanism, the empirical technique developed herein is capable of retrieving coefficients to account for the presence of big drops. If attenuating cells with big drops are present, then larger differences in Z_H (Z_{DR}) over a 5-min period at farther regions will be observed for a given value of Φ_{DP}. Larger a (b) coefficients will be derived and then may be used subsequently to correct values of Z_H (Z_{DR}). It is noted, however, that the retrieved coefficients in these regions may have the effect of overcorrecting Z_H and Z_{DR} data that do not contain big drops. Last, there is a linear correlation between the a and b coefficients from case to case of 0.75. These are derived independently, and empirical evidence presented here confirms prior correlations discovered through simulations.

The dependence of retrieved coefficients on temperature is shown in Fig. 3b. Coefficients would adapt accordingly in the developed scheme if there were indeed a strong sensitivity to temperature. Similar to the scenario presented above with big drops, larger changes in Z_H (Z_{DR}) for a given value of Φ_{DP} would be observed over a 5-min period behind regions of anomalously cold raindrops. The retrieved coefficients would therefore be greater at colder temperatures. However, this effect is not evident in Fig. 3b. It is possible that the temperature dependence of coefficients has been overshadowed by the strong dependence on drop sizes.

4. Validation of retrieved attenuation and differential attenuation coefficients at C band

a. Variables evaluated as a function of Φ_{DP}

If we are to assume that the distribution of Z_H and Z_{DR} is independent of range from radar location and

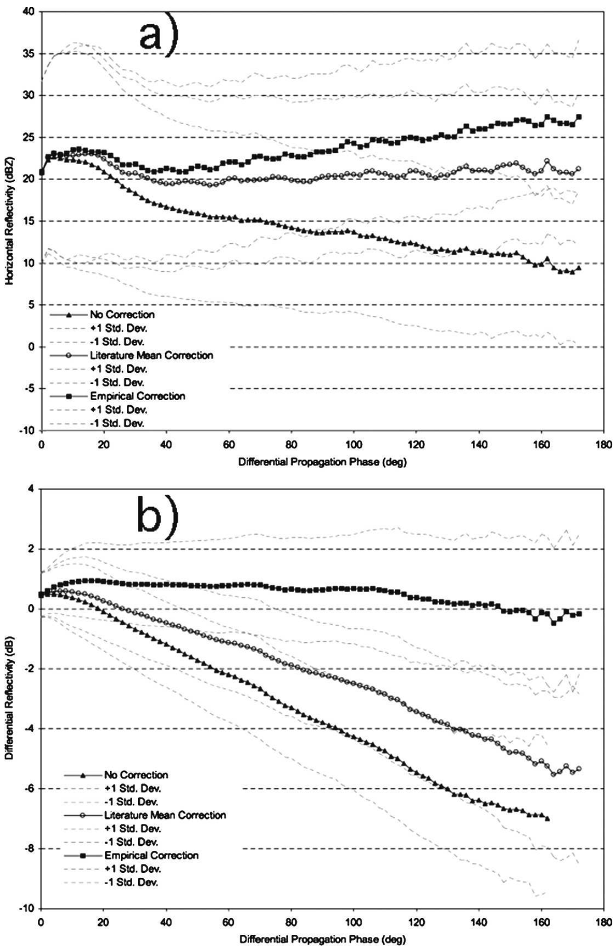

FIG. 4. (a) Mean reflectivity and (b) differential reflectivity with no correction, a literature-mean correction, and the empirically retrieved attenuation coefficients applied to data collected at an elevation angle of 1.5° from 1500 to 1700 UTC 23 Jun 2005.

there is no attenuation, then both variables should also be independent of Φ_{DP} measurements. The validity of this assumption increases with stratiform precipitation, which is more spatially homogeneous than in convection, and for a long duration of analysis. Analyzing corrected and uncorrected Z_{DR} and Z_H as a function of Φ_{DP} serves as a tool for evaluating the accuracy of the retrieved coefficients, whereas it is the basis of deriving *a* and *b* coefficients in the Carey et al. (2000) method. Matrosov et al. (2005) adopt a similar strategy but fix their analysis to a ground-clutter pixel where the reflectivity is assumed to be relatively constant.

Figure 4 shows observations of Z_H and Z_{DR} with no correction for attenuation, correction based on a fixed set of coefficients, and correction based on empirically retrieved coefficients plotted as a function of Φ_{DP} for the 23 June 2005 case. The fixed parameters [$a = 0.0688$ dB $(°)^{-1}$ and $b = 0.017\,85$ dB $(°)^{-1}$] come from mean values at C band based on a literature survey reported in Carey et al. (2000). The 23 June 2005 case is of particular interest because the retrieved *a* (*b*) coefficient is 52% (178%) larger than the literature-mean value.

Figure 4a shows the uncorrected Z_H data have a clear decreasing trend with increasing Φ_{DP} that is due to attenuation effects. Reflectivity data corrected using a fixed *a* coefficient have no evident bias as a function of Φ_{DP}. The retrieved *a* coefficient apparently overcorrects Z_H and results in errors as large as 5 dB. It is possible that the intrinsic Z_H increases with Φ_{DP} because the analysis covers only a 2-h duration. However, it is more likely that errors in the developed retrieval method result from a single coefficient being derived and then applied to gates at several ranges and azimuths. The large coefficients retrieved from the method may only be applicable to the regions behind the attenuating cells containing large drops. The application of a mean coefficient to the entire field of observations is a limitation of the retrieval method in its current configuration.

Observations of uncorrected Z_{DR} data for the same event show a similar decreasing trend with increasing values of Φ_{DP} (Fig. 4b). Mean values of Z_{DR} approach -7 dB at Φ_{DP} measurements of 160°. In this case, corrections using the literature-mean *b* coefficient result in Z_{DR} values that are biased too low by at least 5 dB for Φ_{DP} measurements of 160°. The fact that the literature-mean *a* coefficient provides an accurate correction but the *b* coefficient does not suggests that the literature-mean coefficients are not consistent to each other. After Z_{DR} observations have been adjusted using the empirically retrieved *b* coefficient, the data show much less dependence on Φ_{DP}. There is a slight reduction with increasing Φ_{DP}, but it is evident the retrieved *b* offers a significant improvement over the literature-mean coefficient.

b. Radar–disdrometer comparisons

Similar to the analysis employed in Park et al. (2005b), a disdrometer is used to evaluate the accuracy of the attenuation and differential attenuation correction schemes. A laser-optical disdrometer was placed 24 km from the Trappes radar along the 77° azimuth in Parc Montsouris, Paris. The laser precipitation monitor produces a 228-mm-long parallel infrared beam that is received by a photodiode with a lens. The amplitude of the reduction of the received signal is used to calculate the diameter of the particles passing through the beam. Drop spectra are measured every minute by the disdrometer for drops ranging from 0.1875 to 7 mm in diameter. Reflectivity at horizontal and vertical polarization is computed using scattering simulations at C

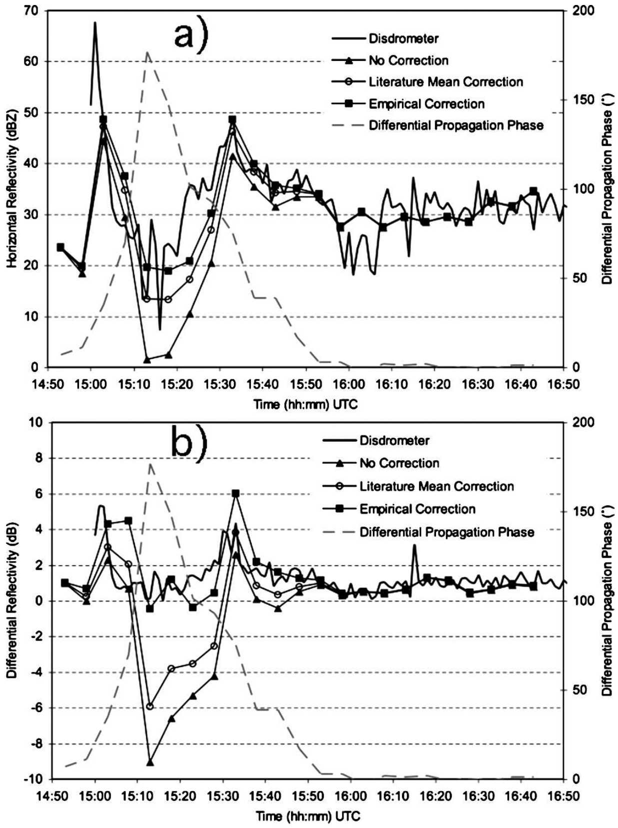

FIG. 5. (a) Reflectivity and (b) differential reflectivity with no correction, a literature-mean correction, and the empirically retrieved attenuation coefficients applied, and compared with collocated disdrometer measurements on 23 Jun 2005.

band. Drop temperatures are assumed to be 15°C and the drop shape model from Goddard et al. (1995) is used. Polarimetric variables computed from disdrometer measurements are subject to errors from the assumed temperature and drop shape model. Another significant source of uncertainty in this analysis comes from the vastly different scales at which disdrometers and radars measure polarimetric quantities. Regardless, simulated values from disdrometer measurements offer an independent measure of Z_H and Z_{DR}.

Figure 5 shows a 2-h time series of radar-measured Z_H and Z_{DR} over the disdrometer that are uncorrected, corrected using fixed parameters, and corrected using retrieved parameters. At 1513 UTC, Φ_{DP} reached 177° over the disdrometer location and subsequently resulted in an attenuated Z_H that was at least 10 dB below simulated values from the disdrometer (Fig. 5a). When the Z_H data have been corrected using a fixed coefficient, measurements agree with simulated values from the disdrometer more closely. However, the best agreement comes from Z_H data that have been corrected with the larger value retrieved using the empirical technique. Figure 4a suggests the retrieved *a* coefficient for the 23 June 2005 case did not improve Z_H measurements over using a fixed coefficient when we consider all data under the radar umbrella. Figure 5a, on the other hand, shows that the retrieved coefficient is more accurate than the fixed value when the analysis is limited to a particular bin that undergoes severe attenuation.

The uncorrected radar measurements of Z_{DR} are attenuated by approximately 9 dB near 1513 UTC (Fig. 5b). Values of Z_{DR} corrected using a fixed *b* value underestimate disdrometer-based measurements by 6 dB during this period of severe differential attenuation. There is almost no bias in comparing disdrometer-based Z_{DR} values with those corrected using the empirically retrieved *b* coefficient. Independent measurements of polarimetric variables afforded by a disdrometer indicate the retrieved coefficients are more accurate than mean coefficients found in the literature for a case of severe attenuation.

c. Radar–radar reflectivity comparisons

There are three, nonpolarimetric C-band radars in the vicinity (Abbeville, Bourges, and Falaise) that operate continuously as part of the French radar network. Measurements from these neighboring radars are used to evaluate objectively the accuracy of retrieved and literature-mean coefficients used to correct Z_H. A similar approach could be implemented for evaluating retrieved *b* coefficients provided the neighboring radars are polarimetric. Reflectivity values from adjacent radars are compared if $\rho_{HV}(0)$ is greater than 0.97 from the Trappes radar, difference in height of measurement is less than 500 m, range to echoes is less than 150 km from both radars, and attenuation from the nonpolarimetric radar is less than 1 dB. The latter criterion is based on a path-integrated Z_H estimation from Doviak and Zrnić (1993).

Reflectivity comparisons are made every 5 min from 0000 to 2345 UTC 24 March 2005, resulting in 1.8×10^5, 5.1×10^4, and 2.6×10^5 data pairs for Trappes and Abbeville, Bourges, and Falaise, respectively. At least 50% of these data pairs were collected at values of $\Phi_{DP} < 10°$ in all cases. Nonzero Z_H differences were noted even at low Φ_{DP} values ($<10°$) for which attenuation effects can be neglected. Gourley et al. (2003) and Tabary (2003) showed that the temporal variability of a radar's calibration can be monitored by comparing Z_H from two different radars. Differences that are not due to attenuation were found by computing the average Z_H difference between Trappes and each neighboring nonpolarimetric C-band radar for $0° < \Phi_{DP} < 10°$ over the duration of the event. Reflectivity differences

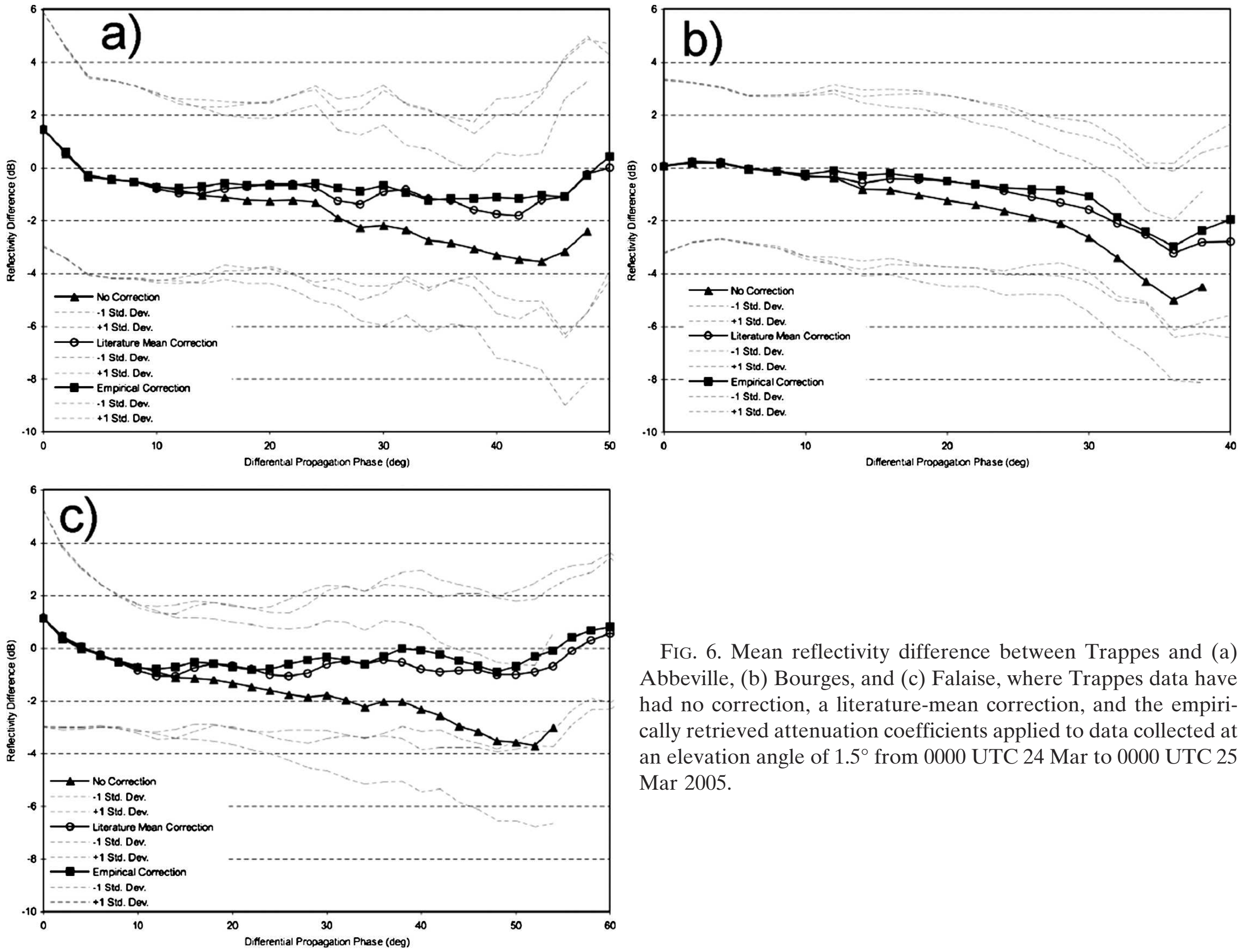

FIG. 6. Mean reflectivity difference between Trappes and (a) Abbeville, (b) Bourges, and (c) Falaise, where Trappes data have had no correction, a literature-mean correction, and the empirically retrieved attenuation coefficients applied to data collected at an elevation angle of 1.5° from 0000 UTC 24 Mar to 0000 UTC 25 Mar 2005.

caused by the combined effects of radar calibration differences and variable beam propagation paths were found to be 1.9, 2.8, and −0.2 dB for Trappes minus Abbeville, Bourges, and Falaise, respectively, and were subsequently subtracted out from all reflectivity differences.

Figure 6 shows uncorrected Z_H values as measured by Trappes minus Z_H from neighboring radars are reduced as Φ_{DP} (a proxy for attenuation) increases. A literature mean coefficient of 0.0688 dB $(°)^{-1}$ and an empirically retrieved coefficient of 0.0805 dB $(°)^{-1}$ were then applied to each Z_H measurement from the Trappes radar and subsequently were compared to all three neighboring radars. In all cases, the mean reflectivity difference is closest to 0 dB when the empirically retrieved coefficient is used to correct for attenuation. It is noted that the estimation of the mean becomes more uncertain as the sample size is reduced. This is especially noticeable at the largest values of Φ_{DP} where the curves exhibit sudden changes.

5. Summary and conclusions

An empirical method has been devised to retrieve coefficients to correct for power losses at C band due to attenuation and differential attenuation in rain. The method relies on the assumption that mean intrinsic values of Z_H and Z_{DR} for each cross-correlated precipitation feature under the radar umbrella do not change when at least 10^4 samples over a 1–2-h duration are considered. Differences between advected and observed values of Z_H and Z_{DR} are linked to changes in Φ_{DP} and enable the empirical retrieval of *a* and *b* attenuation correction coefficients. The retrieved coefficients fall within expectations found through simulations and in other experimental results. Also, the linearity assumption between attenuation and Φ_{DP} was not initially assumed in this method but was found to be valid.

Relationships between retrieved coefficients and characteristics of cells that were responsible for the attenuation were analyzed. It was discovered that larger coefficients for both Z_H and Z_{DR} were empirically retrieved when a relatively large percentage of big drops ($Z_{DR} > 3$ dB at C band) were present. Moreover, the *a* and *b* coefficients were found to be linearly related with a correlation of 0.75. Temperature effects on attenuation, however, were not noticeable but were perhaps masked by the large dependence on the presence of large drops. Changes in raindrop shape or Mie scattering effects are likely culprits for the increased attenuation observed with large-diameter drops.

The accuracy of the retrieved coefficients was evaluated by plotting Z_H and Z_{DR} before and after correction as a function of Φ_{DP}, comparison with disdrometer-based measurements, and comparison with unattenuated data from neighboring radars. Because improvements over uncorrected values were inevitable, a benchmark was established by correcting Z_H and Z_{DR} data using fixed *a* and *b* coefficients from a literature survey at C band. All analyses indicate the empirically retrieved *b* coefficients result in more accurate Z_{DR} values as compared with uncorrected values and those corrected using a fixed coefficient. There is a suggestion that the retrieved *a* coefficient overcorrected Z_H data when considering all observations around the radar. However, when a single pixel over the disdrometer site was examined, better agreement with simulated Z_H from the disdrometer observations was accomplished using the empirically retrieved coefficient. This pixel had an associated Φ_{DP} value of 177° and therefore was severely attenuated. It is plausible that the retrieval method responds to severe attenuation caused by Mie scattering and thus may overcorrect Z_H observations that did not experience these effects.

Several considerations must be made regarding the operational application of this empirical technique. As with other attenuation correction methods, there is no consideration for inflated Z_H values resulting from hail or brightband contamination. These errors will likely grow after attenuation coefficients have been applied. Also, it is noted that the method in its current form does not provide the capability of varying the coefficients in space. Instead, coefficients are applied to entire fields of Z_H and Z_{DR} and thus may overcorrect data that do not contain large drops, for example. Future methods should consider subdividing radar observations that have similar characteristics and then retrieving multiple coefficients. Approximately 1–2 h of data were needed to retrieve the coefficients successfully. These hours were typically characteristic of large wedges of Φ_{DP} that rotated rapidly in the azimuthal direction, resembling a searchlight. Data pairs are considered in the retrieval method if their values of Φ_{DP} differ by at least 10°. It will be more difficult to meet this criterion in stratiform rain that has a more homogeneous spatial structure.

Acknowledgments. This work was done in the frame of the Projet Application Radar à la Météorologie Infra-Synoptique (ARAMIS) Nouvelles Technologies en Hydrométéorologie Extension et Renouvellement (PANTHERE) supported by Météo-France, the French "Ministère de L'Écologie et du Développement Durable," the "European Regional Development Fund (ERDF)" of the European Union, and CEMAGREF. The authors would like to acknowledge the advice provided by the PANTHERE scientific review committee. Specifically, Anthony Illingworth provided us with many useful insights regarding attenuation correction methods, and he helped with the review of this paper. Kim Dokhac was helpful in processing the disdrometer data. The comments from three anonymous reviewers greatly improved the quality of this manuscript. Their assistance is greatly appreciated.

REFERENCES

Anagnostou, E. N., M. N. Anagnostou, W. F. Krajewski, A. Kruger, and B. J. Miriovsky, 2004: High-resolution rainfall estimation from X-band polarimetric radar measurements. *J. Hydrometeor.,* **5,** 110–128.

Aydin, K., Y. Zhao, and T. A. Seliga, 1989: Rain-induced attenuation effects on C-band dual-polarization meteorological radars. *IEEE Trans. Geosci. Remote Sens.,* **27,** 57–66.

Bringi, V. N., and V. Chandrasekar, 2001: *Polarimetric Doppler Weather Radar: Principles and Applications.* Cambridge University Press, 636 pp.

——, ——, N. Balakrishnan, and D. S. Zrnić, 1990: An examination of propagation effects in rainfall on radar measurements at microwave frequencies. *J. Atmos. Oceanic Technol.,* **7,** 829–840.

Carey, L. D., S. A. Rutledge, D. A. Ahijevych, and T. D. Keenan, 2000: Correcting propagation effects in C-band polarimetric radar observations of tropical convection using differential propagation phase. *J. Appl. Meteor.,* **39,** 1405–1433.

Doviak, R. J., and D. Zrnić, 1993: *Doppler Radar and Weather Observations.* Academic Press, 562 pp.

Goddard, J. W. F., K. L. Morgan, A. J. Illingworth, and H. Sauvageot, 1995: Dual-wavelength polarization measurements in precipitation using the CAMRA and Rabelais radars. Preprints, *27th Conf. on Radar Meteorology,* Vail, CO, Amer. Meteor. Soc., 196–198.

Gorgucci, E., G. Scarchilli, and V. Chandrasekar, 1995: Radar and raingage measurements of rainfall over the Arno basin. Preprints, *Conf. on Hydrology,* Dallas, TX, Amer. Meteor. Soc., 68–73.

——, ——, ——, P. F. Meischner, and M. Hagen, 1998: Intercomparison of techniques to correct for attenuation of C-band weather radar signals. *J. Appl. Meteor.,* **37,** 845–853.

Gourley, J. J., B. Kaney, and R. A. Maddox, 2003: Evaluating the calibrations of radars: A software approach. Preprints, *31st Conf. on Radar Meteorology,* Seattle, WA, Amer. Meteor. Soc., 459–462.

——, P. Tabary, and J. Parent du Chatelet, 2006: Data quality of the Météo-France C-band polarimetric radar. *J. Atmos. Oceanic Technol.,* **23,** 1340–1356.

Hitschfeld, W., and J. Bordan, 1954: Errors inherent in radar measurement of rainfall at attenuating wavelengths. *J. Meteor.,* **11,** 58–67.

Iwanami, K., E. Le Bouar, J. Testud, M. Maki, R. Misumi, S.-G. Park, and M. Suto, 2003: Application of the rain profiling algorithm ZPHI to the X-band polarimetric radar data observed in Japan. Preprints, *31st Conf. on Radar Meteorology,* Seattle, WA, Amer. Meteor. Soc., 274–276.

Jameson, A. R., 1992: The effect of temperature on attenuation-correction schemes in rain using polarization propagation differential phase shift. *J. Appl. Meteor.,* **31,** 1106–1118.

Matrosov, S. Y., K. A. Clark, B. E. Martner, and A. Tokay, 2002: X-band polarimetric radar measurements of rainfall. *J. Appl. Meteor.,* **41,** 941–952.

——, D. E. Kingsmill, B. E. Martner, and F. M. Ralph, 2005: The utility of X-band polarimetric radar for quantitative estimates of rainfall parameters. *J. Hydrometeor.,* **6,** 248–262.

Park, S.-G., V. N. Bringi, V. Chandrasekar, M. Maki, and K. Iwanami, 2005a: Correction of radar reflectivity and differential reflectivity for rain attenuation at X band. Part I: Theoretical and empirical basis. *J. Atmos. Oceanic Technol.,* **22,** 1621–1632.

——, M. Maki, K. Iwanami, V. N. Bringi, and V. Chandrasekar, 2005b: Correction of radar reflectivity and differential reflectivity for rain attenuation at X band. Part II: Evaluation and application. *J. Atmos. Oceanic Technol.,* **22,** 1633–1655.

Rinehart, R. E., 1979: Internal storm motions from a single non-Doppler weather radar. NCAR Tech. Note NCAR/TN-146+STR, 262 pp.

Ryzhkov, A. V., and D. S. Zrnić, 1995: Precipitation and attenuation measurements at a 10-cm wavelength. *J. Appl. Meteor.,* **34,** 2121–2134.

Smyth, T. J., and A. J. Illingworth, 1998: Correction for attenuation of radar reflectivity using polarisation data. *Quart. J. Roy. Meteor. Soc.,* **124,** 2393–2415.

Tabary, P., 2003: Efforts to improve the monitoring of the French radar network. Preprints, *31st Conf. on Radar Meteorology,* Seattle, WA, Amer. Meteor. Soc., 482–485.

Testud, J., E. Le Bouar, E. Obligis, and M. Ali-Mehenni, 2000: The rain profiling algorithm applied to polarimetric weather radar. *J. Atmos. Oceanic Technol.,* **17,** 332–356.

Tuttle, J. D., and G. B. Foote, 1990: Determination of the boundary layer airflow from a single Doppler radar. *J. Atmos. Oceanic Technol.,* **7,** 218–232.

Zrnić, D. S., and A. Ryzhkov, 1996: Advantages of rain measurements using specific differential phase. *J. Atmos. Oceanic Technol.,* **13,** 454–464.